



## ORIGINAL ARTICLE

# Establishment and characterization of patient-derived high-grade glioma cell lines, and validation of their tumorigenicity in murine xenograft model

Natália Barreto<sup>1</sup>, Valquiria Aparecida Matheus<sup>1</sup>, Ingrid Mayara Cavalcante Trevisan<sup>1</sup>, Thaís Tuasca Jareño<sup>2</sup>, Giovanna Marques Antunes<sup>2</sup>, Julio Cesar de Moraes<sup>3</sup>, Liana Verinaud<sup>4\*</sup>, Jean Gonçalves de Oliveira<sup>2</sup>, José Carlos Esteves Veiga<sup>2</sup>, João Luiz Vitorino-Araujo<sup>2</sup>, Catarina Rapôso<sup>1\*</sup>

<sup>1</sup>Faculty of Pharmaceutical Sciences, University of Campinas, Campinas, São Paulo, Brazil, <sup>2</sup>Division of Neurosurgery, Department of Surgery, Santa Casa de São Paulo School of Medical Sciences, São Paulo, Brazil, <sup>3</sup>Imunocel Laboratory, Campinas, São Paulo, Brazil, <sup>4</sup>Department of Structural and Functional Biology, Biology Institute, University of Campinas, Campinas, São Paulo, Brazil

## ARTICLE INFO

*Article history:*

Received: June 14, 2024

Accepted: October 8, 2024

Published Online: December 5, 2024

*Keywords:*

High-grade gliomas

Cancer cell lines

Human primary cell line

Glioblastoma

Tumorigenicity

*\*Corresponding authors:*

Catarina Rapôso

Faculty of Pharmaceutical Sciences, University of Campinas, Campinas, São Paulo, Brazil.

Email: raposo@unicamp.br

Liana Verinaud

Department of Structural and Functional Biology, Biology Institute, UNICAMP, Campinas, São Paulo, Brazil.

Email: verinaud@unicamp.br

© 2024 Author(s). This is an Open-Access article distributed under the terms of the Creative Commons Attribution-Noncommercial License, permitting all non-commercial use, distribution, and reproduction in any medium, provided the original work is properly cited.

## ABSTRACT

**Background:** Diffuse high-grade gliomas (HGGs) include the most aggressive types of brain tumors. Despite current treatment options, which include a combination of surgery, radiotherapy, and chemotherapy, the prognosis remains catastrophic. Patients diagnosed with glioblastoma (GB), the most aggressive HGG, have a median survival of <2 years. Cancer cell lines represent an essential tool in cancer research. Once established, these cells can be used to investigate tumor biology and conduct drug screening trials, contributing to the development of new therapeutic options for patients with glioma.

**Aim:** The aim of the study was to establish and characterize three new HGG cell lines obtained from different patients and validate their tumorigenicity in a murine xenograft model.

**Methods:** The three tissue samples were immunohistochemically and molecularly classified as astrocytoma IDH-mutant, Grade 3 (C03); GB IDH-wildtype, grade 4 (N07); and astrocytoma IDH-mutant, Grade 3 (L09). These were cultured until the tenth passage for culture establishment. Cell morphology was accessed by light microscopy and phalloidin labeling. To characterize the cell lines, GFAP labeling was performed. Xenograft murine models were used to investigate whether the cell lines retained their tumor-forming ability. Cells from murine tumors were recultured, and morphological evaluation was performed by histopathological analysis.

**Results:** The three HGG lines were successfully established, and GFAP positivity confirmed their astrocytic origin. Morphologically, the cells presented a fusiform or polygonal shape, with accelerated growth throughout the passages. All three cell lines developed tumors after induction of the xenograft model, and the subculture of these tumors revealed a morphology similar to that of the three cell lines before implantation. Histopathological analysis of the xenograft tumors confirmed the disordered tissue formation commonly found in diffuse gliomas.

**Conclusion:** The successful establishment of these cell lines and the creation of a biobank will facilitate studies in drug development and glioma tumorigenesis.

**Relevance for Patients:** The established cell lines will be utilized in assays to analyze glioma tumorigenesis and in screening for novel drug candidates, contributing to the development of new treatments for these patients.

## 1. Introduction

Diffuse high-grade gliomas (HGGs) are a heterogeneous group of tumors that originate from glial or glial precursor cells and are among the most aggressive and prevalent

brain tumors in adults [1]. According to the 2021 World Health Organization (WHO) Classification of Tumors of the Central Nervous System (WHO CNS5), adult diffuse gliomas are classified into: (i) Astrocytoma, IDH-mutant (grades 2, 3, or 4), (ii) oligodendroglioma, IDH-mutant, and 1p/19q-codeleted (grades 2 or 3); and (iii) glioblastoma (GB), IDH-wildtype (grade 4) [2]. CNS WHO Grades 1 – 4 are related to the degree of malignancy, with a higher grade corresponding to a poorer prognosis [2-4]. Standard treatments for HGGs involve a combination of maximal surgical resection, radiotherapy, and chemotherapy [5,6]. However, these treatments have limited efficacy in preventing glioma progression. GB is the most common and highly malignant type of brain tumor in adults, with a median survival of <2 years for most patients [7,8]. Given the poor outcomes associated with HGGs, there is a need to explore new therapeutic approaches or even improve the efficacy of conventional therapies against these tumors.

Patient-derived cancer cell lines are the most commonly used models to study tumor biology and discover novel therapeutics, not only *in vitro* but also in murine *in vivo* assays [9,10]. Once established, malignant cell cultures provide excellent and permanent materials for studying tumor biology and behavior. They facilitate the analysis of bioactive components produced by tumors, the determination of cell viability and proliferation, and the assessment of cell migration and invasion under treatment conditions [11]. Therefore, *in vitro* assays are a fundamental step in drug development, as they permit screening for agents that selectively target tumors. For example, the successful establishment of a human GB cell line (named NG97) [11,12] allowed our research group to identify spider venom molecules with antitumor effects [3,13-16]. These studies emphasize the importance of establishing cancer cell lines. However, their focus primarily remained on one glioma cell type (GB-NG97). Considering the heterogeneity of gliomas, trials involving multiple cell types from different patients could provide a more comprehensive understanding of the effects of animal venom molecules on these tumors.

Despite being an excellent model for cancer research and drug development, establishing cell lines from fresh tissue obtained from patients is time-consuming and challenging. In contrast to established cell lines, primary cells are sensitive to new environments and more susceptible to contamination. Bian *et al.* [17] reported that the success rate of cell line establishment from fresh tumor tissues is around 10%. In the present study, we aimed to establish and characterize three new human cell lines derived from fresh tissue samples of three male patients diagnosed with HGGs. Through a simple yet carefully optimized process, we aimed to establish the cell lines after only a few passages, ensuring they became stable while remaining as close as possible to the original tumor tissue. These newly established cell lines will facilitate future studies related to the understanding of glioma biology, especially due to their distinct histological and molecular characteristics. These cell lines will also enable our research group to conduct new tests investigating the effects of animal venom molecules. A well-established tumor cell bank provides heterogeneous cell lines

and opens perspectives for studies aimed at developing new treatments against these tumors.

## 2. Methods

### 2.1. Ethical considerations

Tissue samples were obtained from the department of neurosurgery and imaging examinations were acquired from the department of radiology, both at the Central Hospital of Santa Casa (Brazil) after informed patient consent (Termo de Consentimento Livre e Esclarecido [TCLE]). Tumor samples were acquired following the ethical guidelines of the Research Ethics Committee of the University of Campinas (UNICAMP, Brazil; CAAE: 15215219.5.0000.5404) and the Central Hospital of Santa Casa (Brazil; CAAE: 15215219.5.3001.5479). Animal experiments were performed in accordance with the Ethical Principles in Animal Research, adopted by the Brazilian College of Animal Experimentation (Colégio Brasileiro de Experimentação Animal [COBEA]); all procedures were previously approved by the Animal Use Ethics Committee (CEUA/UNICAMP; 6200-1/2023). The animals were carefully monitored and cared for daily to ensure their well-being. They were kept in standard filter-top cages with unrestricted access to sterile water and food in the Animal Facility of the Institute of Biology, Department of Functional and Structural Biology (UNICAMP).

### 2.2. Specimen collection

After surgical resection, tissue samples were obtained from three different patients: a 55-year-old male (specimen designated C03), a 56-year-old male (N07), and a 36-year-old male (L09). Under aseptic conditions, a portion of the samples from each patient was placed in separate falcon tubes containing Iscove's Modified Dulbecco's Medium (IMDM; #17633; Sigma-Aldrich, United States of America [USA]) supplemented with 10% fetal bovine serum (FBS) and penicillin-streptomycin-amphotericin B solution (10.000 U/mL; #A5955; Sigma-Aldrich, USA) (pH 7.4) (referred to as complete medium). These samples were intended for the preparation of primary cell cultures. The remaining portions were placed in other falcon tubes containing 10% formaldehyde and sent to a histopathology laboratory, where the tumors were characterized immunohistochemically and molecularly according to WHO CNS5 2021, as follows: astrocytoma IDH-mutant, WHO Grade 3 (C03); GB IDH-wildtype, WHO grade 4 (N07); and astrocytoma IDH-mutant, WHO Grade 3 (L09).

### 2.3. Cell lines establishment

Tumor specimens were maintained in a complete medium, minced into 1 – 2 mm<sup>3</sup> fragments, and centrifuged (1500 rpm, 4°C, 5 min) to remove debris. The supernatant was then discarded, and the cells (pellet) were seeded into 25 cm<sup>2</sup> culture bottles. Primary cells were cultured (IMDM) and maintained at 37°C in a 5% CO<sub>2</sub> humidified atmosphere until they reached the tenth passage. Each passage involves releasing the cells from the bottle using a cell scraper and transferring them to a larger bottle or two other bottles. By the tenth passage, the cells were observed to be stable after thawing, indicating successful

establishment. Large quantities of the three cell lines were then routinely frozen at  $-80^{\circ}\text{C}$  in FBS supplemented with 10% (v/v) dimethyl sulfoxide (DMSO; #D2650; Sigma-Aldrich, USA) and stored long-term in a cryogenic freezer within liquid nitrogen vapor (biobank). For the immunofluorescence assay, cells were thawed, cultured, and allowed to reach 90% confluence before being carefully scraped into 48-well plates (Corning Costar®, USA). In addition,  $3 \times 10^5$  cells were also obtained for the tumorigenicity assay as described below.

#### 2.4. Immunofluorescence

Characterization and authentication of the three established cell lines were assessed using immunostaining for glial fibrillary acidic protein (GFAP), an astrocyte marker. Cell morphology was also assessed using phalloidin to selectively label actin filaments. This assay was based on a standardized protocol in our laboratory, which was described in a previous study [13]. Cells were initially seeded in 48-well plates ( $2 \times 10^5$  cells/well) with a complete medium. At 90% confluence, the medium was removed from the wells and replaced with fresh medium. Cells were then fixed with 4% paraformaldehyde (PFA) (15 min), washed three times with phosphate-buffered saline (PBS) (pH 7.4), and incubated with a permeabilization solution (0.1% Triton X-100 in PBS) for 10 min at room temperature. After, the wells were washed with PBS and then treated with a blocking solution (1% bovine serum albumin [BSA] 467 supplemented 0.2% Tween 20 in PBS) for 1 h. Subsequently, the cells were incubated with a Phalloidin probe (1:200, P5282; Sigma-Aldrich, USA) diluted in 0.3% BSA solution (supplemented with 0.1% Tween 20 in PBS) for 2 h at room temperature. Following this, the wells were washed with PBS and incubated overnight with anti-GFAP (1:500; #16825-I-AP; Proteintech, USA) in the same dilution solution. A negative control group without anti-GFAP incubation was also prepared. The next day, cells were washed again with PBS and incubated with rhodamine (TRITC) – conjugated goat anti-rabbit IgG (1:100; #SA00007-2; Proteintech, USA) for 1 h, and then counterstained with a drop of the nucleus dye DAPI (#P36971; ThermoFisher, USA). Cell imaging was performed using Apotome.2 (Zeiss, Germany) and analyzed with Zen 2.6 and Image J software.

#### 2.5. Tumorigenicity in $RAG^{-/-}$ black mice

To investigate tumorigenicity,  $3 \times 10^5$  cells from each of the three cell lines were suspended in 0.1 mL PBS and injected subcutaneously into the dorsal flank of adult immunodeficient C57BL/6  $RAG^{-/-}$  female or male mice (12 months old). The animals were monitored weekly during tumor development. After 22 days of cell implantation, the mice were anesthetized with ketamine (80 mg/kg) and xylazine (10 mg/kg) and euthanized. Tumors were excised and divided into two parts for different processing methods. One part was fixed in 4% PFA and embedded in paraffin for tissue analysis by hematoxylin and eosin (H&E) staining. The other part was placed in a falcon tube containing a complete medium for subculture, morphological analysis, and creation of a biobank.

#### 2.6. Tumor histopathology

Tumor pieces designated for tissue analysis were immersed in PFA for 24 h. Thereafter, the tissue pieces were washed with distilled water 3 times (10 min each) to remove any residual PFA. The samples were then dehydrated through an ethanol gradient and embedded in Paraplast (#P3558; Sigma-Aldrich, USA). Sections of 5  $\mu\text{m}$  were obtained and stained with H&E before evaluation under a microscope.

#### 2.7. Morphological evaluation

For evaluation of morphology, the three established cell lines (obtained from patients) and those acquired after tumor excision from mice were seeded in 6-well plates ( $2 \times 10^5$  cells/well) and incubated at  $37^{\circ}\text{C}$ , 5%  $\text{CO}_2$  for 48 h. The cells were then photographed under an inverted microscope (Nikon Eclipse Ts2; Nikon, Japan) and the NIS-Elements D software to analyze their general morphology. The entire methodology used in this work is summarized and exemplified in Figures 1A and B.

### 3. Results

#### 3.1. Establishment and biobanking of the three high-grade glioma cell lines from patient tumor tissues and morphological evaluation

A tumor mass was observed in the MRI of the patient before surgery (Figures 2A, 3A, and 4A). Using *in vitro* patient-derived specimens, the three HGG cell lines (C03, N07, and L09) were successfully established. From the primary culture, it was possible to freeze, thaw, and subculture cells, allowing the creation of a biobank and the performance of *in vitro* characterization (GFAP labeling), as described below. During the first 2 weeks of culture, the GB (N07) cell line grew faster than the astrocytoma (C03 and L09) cell lines. Later, growth was similar for all three HGG cell lines. All of them reached the tenth passage in about 2 months. Under light microscopy, all three cell lines grew in monolayer and most of them exhibited spindle-shaped and polygonal morphologies; some of them exhibited long protrusions (Figures 2B, 3B, and 4B).

#### 3.2. Tumorigenicity of the three high-grade glioma cell lines in C57BL/6 $RAG^{-/-}$ mice and morphological evaluation

To assess whether the three cell lines retained their tumor-forming ability, a tumorigenicity assay was conducted. *In vivo*, xenograft tumors were developed after subcutaneous implantation of all three established cell lines (Figures 2C and D; 3C and D; and 4C; and D). After 22 days of inoculation, the animals were anesthetized and the tumor masses were excised. The tumors reached a volume of 2.5, 0.7, and 2.02  $\text{cm}^3$ , with weights of 1.6, 0.8, and 1.5 g, respectively (for C03, N07, and L09). The morphology of the xenograft tumors during subculture resembled the cell line characteristics of the three cell lines before implantation, displaying spindle-shaped and polygonal morphologies (Figures 2E, 3E, and 4E).

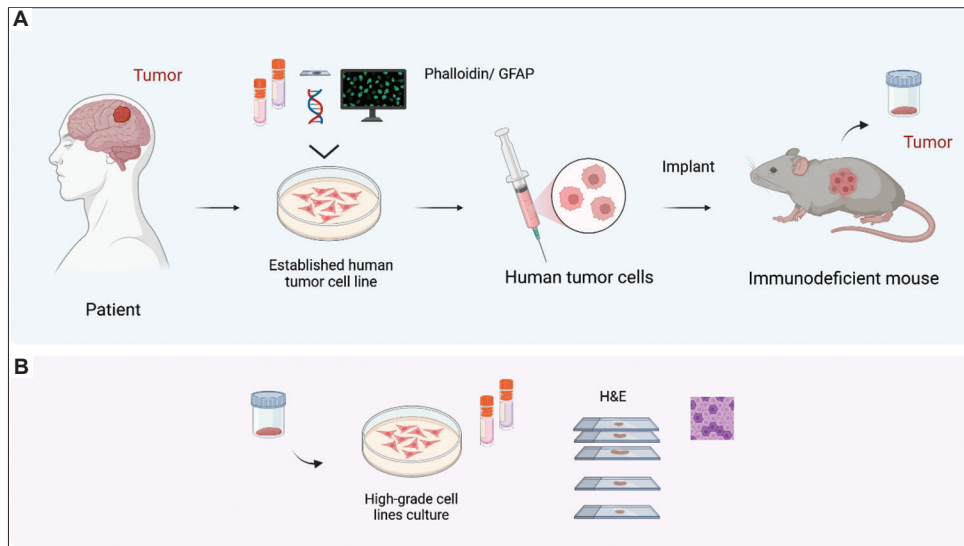


**Figure 1.** Methodology summary. Establishment of patient-derived high-grade glioma cell lines (C03, N07, and L09), and *in vivo* tumorigenicity analysis. (A) After patient consent, portions of the obtained tumor samples were cultured until they reached the tenth passage (establishment). Large amounts of these cells were frozen to create a biobank. Morphological analysis and characterization of the cell lines (GFAP labeling) were performed using an inverted microscope and immunofluorescence assays, respectively. The remaining tumor portions were destined for histopathological and molecular classification. Subsequently, the cell lines were implanted in a xenogeneic murine model to evaluate their tumor-forming capacity. (B) Fragments of the tumors developed and excised from the animals were sub-cultivated for their establishment and for creating another biobank. Other tumor fragments were processed for histopathological evaluation (H&E staining). GFAP: Glial fibrillary acidic protein; H&E: Hematoxylin and eosin. The figure was created in BioRender; Santos, N. (2023; <https://BioRender.com/w44p823>)

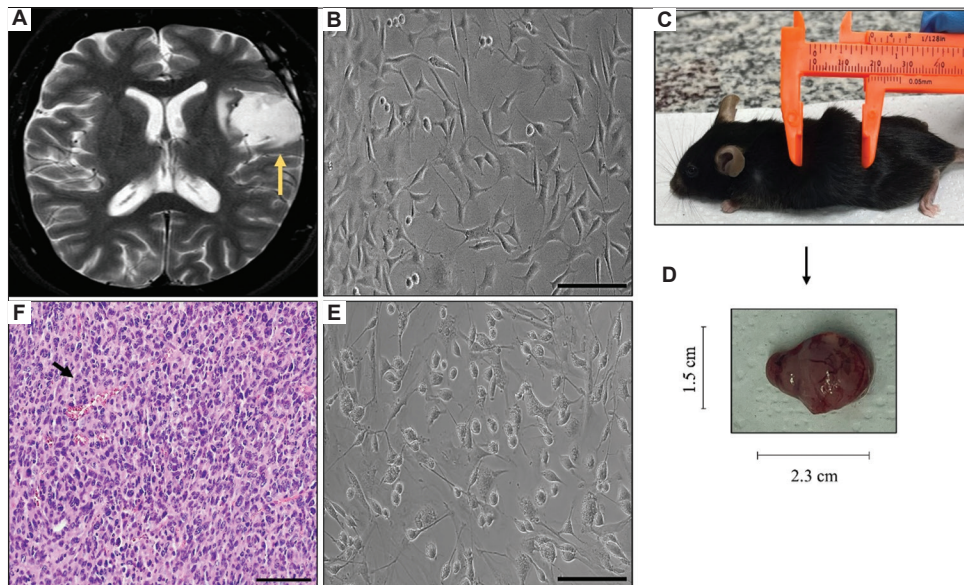


**Figure 2.** Astrocytoma IDH-mutant, grade 3 (C03) human cells. (A) MRI of the patient before surgery; the tumor mass is indicated with a yellow arrow. (B) C03 cell line during its culture and establishment. The cell line was observed under an inverted microscope after the tenth passage, exhibiting spindle-shaped and polygonal morphologies; some exhibiting long protrusions. (C) Tumorigenicity test of C03 in C57BL/6 RAG<sup>-/-</sup> mice. (D) The solid tumor obtained (volume: 2.5 cm<sup>3</sup>; weight: 1.6 g). (E) C03 cell line during its culture after excision of the animal's tumor. Note that their morphology resembles that of the C03 cell line before implantation. (F) Histopathology (H&E) of the subcutaneous tumor, displaying increased cellularity, variation in nuclear size, and mitotic figures (black arrow). Scale bars: 100  $\mu$ m (B and E); 50  $\mu$ m (F) Abbreviations: MRI: Magnetic resonance imaging; H&E: Hematoxylin and eosin

### 3.3. Histopathology of tumor mass

Histopathological examination was performed to assess whether the xenografted tumors retained features observed

in astrocytic tumors. Tumors originating from all three cell lines indicated increased cellularity, variation in nuclear size, and mitotic figures, similar to astrocytic tumors (Figures 2F, 3F, and 4F).

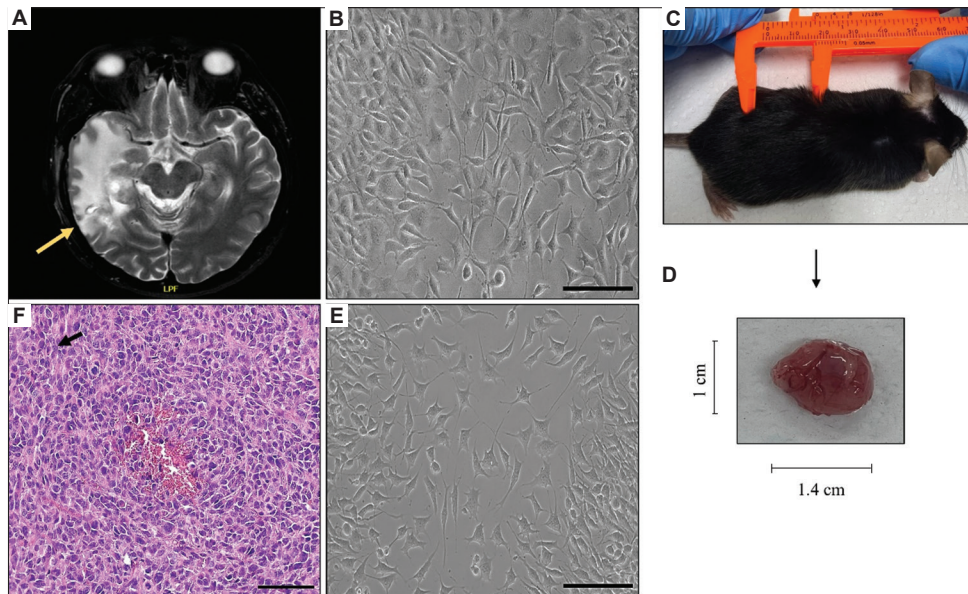


**Figure 3.** Glioblastoma IDH-wildtype, Grade 4 (N07) human cells. (A) MRI of the patient before surgery; the tumor mass is indicated with a yellow arrow. (B) N07 cell line during its culture and establishment. The cell line was observed under an inverted microscope after the tenth passage, exhibiting spindle-shaped and polygonal morphologies; some exhibiting long protrusions. (C) Tumorigenicity test of N07 in C57BL/6 RAG<sup>-/-</sup> mice. (D) The solid tumor obtained (volume: 0.7 cm<sup>3</sup>; weight: 0.8 g). (E) N07 cell line during its culture after excision of the animal's tumor. Note that their morphology resembles that of the N07 cell line before implantation. (F) Histopathology (H&E) of the subcutaneous tumor, displaying increased cellularity, variation in nuclear size, and mitotic figures (black arrow). Scale bars: 100 μm (B and E); 50 μm (F). Abbreviations: MRI: Magnetic resonance imaging; H&E: Hematoxylin and eosin

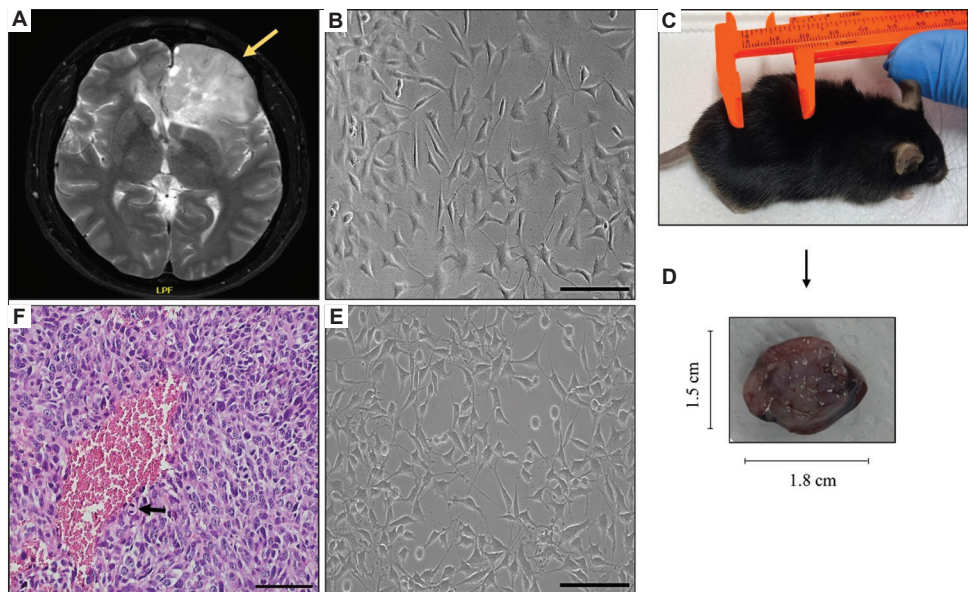


**Figure 4.** Astrocytoma IDH-mutant, Grade 3 (L09) human cells. (A) MRI of the patient before surgery; the tumor mass is indicated with a yellow arrow. (B) L09 cell line during its culture and establishment. The cell line was observed under an inverted microscope after the tenth passage, exhibiting spindle-shaped and polygonal morphologies; some exhibiting long protrusions. (C) Tumorigenicity test of L09 in C57BL/6 RAG<sup>-/-</sup> mice. (D) The solid tumor obtained (volume: 2.02 cm<sup>3</sup>; weight: 1.5 g). (E) L09 cell line during its culture after excision of the animal's tumor. Note that their morphology resembles that of the L09 cell line before implantation. (F) Histopathology (H&E) of the subcutaneous tumor, displaying increased cellularity, variation in nuclear size, and mitotic figures (black arrow). Scale bars: 100 μm (B and E); 50 μm (F). Abbreviations: MRI: Magnetic resonance imaging; H&E: Hematoxylin and eosin

### 3.4. Phalloidin and GFAP labeling

To characterize and authenticate the three established cell lines, immunostaining for GFAP, a reliable marker of astrocytic cells, was performed. Immunofluorescence was also carried out

to evaluate glioma cell morphology by phalloidin labeling. All three HGG cells displayed a rounded morphology with some thin extensions. GFAP labeling was positive in all HGGs, confirming their astrocytic origin (Figures 5A-D, 6A-D, and 7A-D).

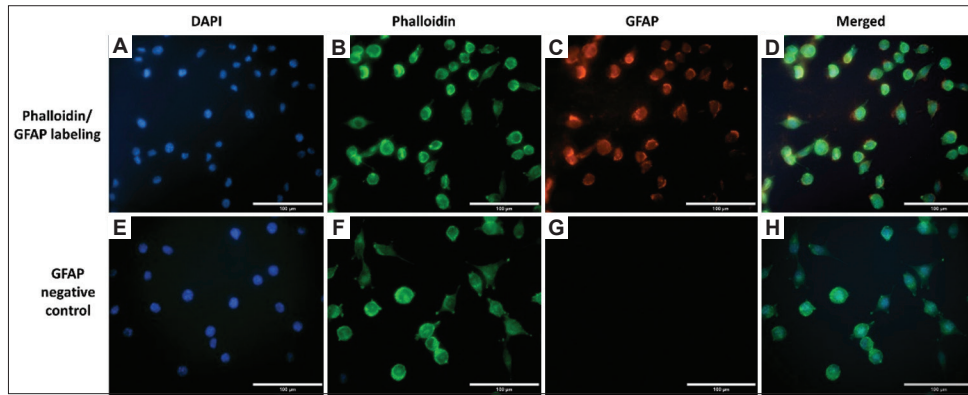


**Figure 5.** Astrocytoma IDH-mutant, Grade 3 (C03) human cells. (A-D) Phalloidin probe and GFAP labeling. The cells displayed rounded morphology with some thin extensions; GFAP staining was positive in C03 cells, confirming astrocytic origin. (E-H) Negative control (without GFAP labeling). Scale bars: 100 µm

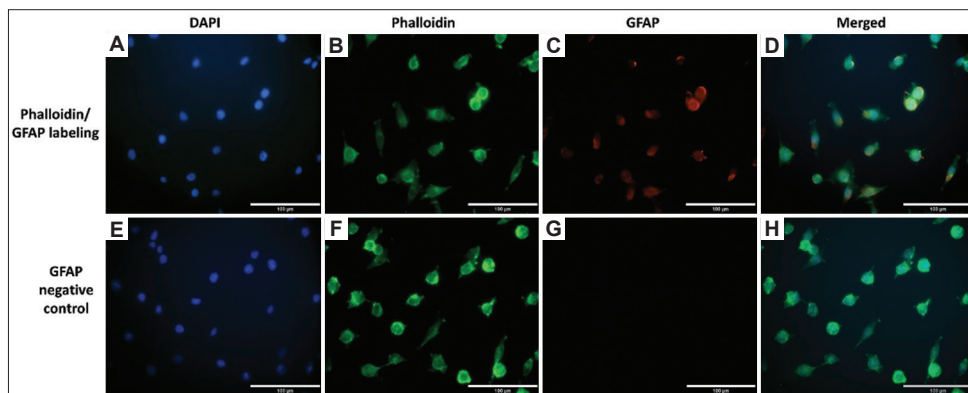


**Figure 6.** Glioblastoma IDH-wildtype, Grade 3 (N07) human cells. (A-D) Phalloidin probe and GFAP labeling. The cells displayed rounded morphology with some thin extensions; GFAP staining was positive in N07 cells, confirming astrocytic origin. (A-H) Negative control (without GFAP labeling). Scale bars: 100 µm

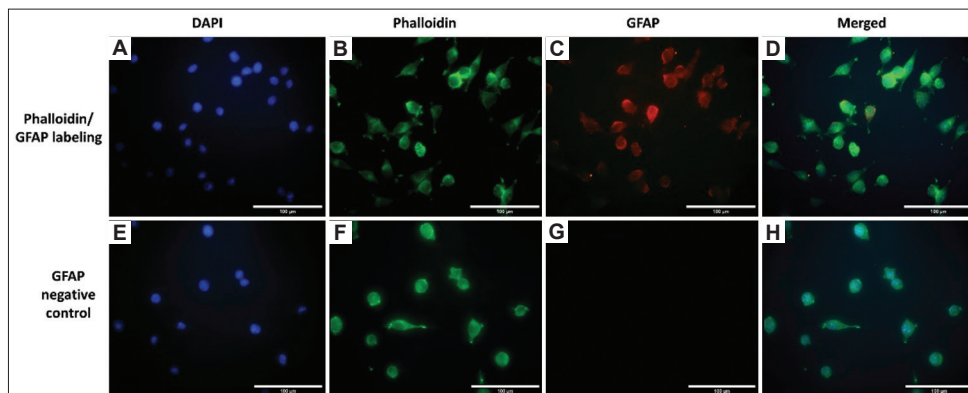


**Figure 7.** Astrocytoma IDH-mutant, grade 3 (L09) human cells. (A-D) Phalloidin probe and GFAP labeling. The cells displayed rounded morphology with some thin extensions; GFAP staining was positive in L09 cells, confirming astrocytic origin. (E-H) Negative control (without GFAP labeling). Scale bars: 100 µm

Negative controls (without GFAP labeling) were also performed (Figures 5E-H, 6E-H, and 7E-H).

#### 4. Discussion

Cancer cell lines are one of the most powerful tools in cancer research. Establishing new primary cancer cell lines obtained

directly from patient tumor tissue is essential to understanding tumor behavior and biology, as well as establishing a preclinical model for testing and developing new drugs [10,18]. These cell lines are commonly used to assess drug sensitivity, resistance, and toxicity. However, after numerous passages, these cell lines can accumulate genetic and epigenetic changes that may

hinder many preclinical studies from translating into clinical applications. The occurrence of multiple passages makes these cell lines less similar to the original tissue [19,20]. This allows newly established cell lines to become a better study model than commercially available cell lines. In the present study, we were able to establish three new HGG cell lines (C03, N07, and L09) after 10 passages, obtained directly from primary tumors of different patients. During the adaptation period, astrocytoma cell lines (C03 and L09) slowly adhered to the culture flasks and began to proliferate more rapidly until reaching the tenth passage. Interestingly, the GB cell line (N07) grew faster in the first 2 weeks of culture than the astrocytomas. Thereafter, growth was similar for all three HGG cell lines. These differences may be related to GB being a more aggressive tumor; however, after the 2<sup>nd</sup> week, its growth remained similar to that of the other cell lines. After reaching the tenth passage (approximately 2 months), it was noted that they became stable after thawing.

Compared to other cell culture models, like sphere culture, adherent cells are easy to manipulate and are ideal for drug screening experiments, such as cell proliferation, viability, and migration assays. Although easy to manipulate, primary cultures are more susceptible to contamination. They are also more sensitive to microenvironmental components, making the choice of an appropriate culture medium essential. Cheng *et al.* [21] cultured 10 GB cell lines from different patients using high-glucose DMEM + 10% FBS, but only one of them (GWH04) acquired unlimited proliferation capacity. In the present study, all three HGG cell lines acquired stability and high replicative ability with complete medium (IMDM + 10% FBS), without the need for additional glucose supplementation. Morphological analysis is commonly used to assess the characteristics of cancer cell lines. Despite being different types of gliomas, all three HGG cell lines grew in a monolayer and exhibited spindle-shaped and polygonal morphologies. These morphological findings are in agreement with studies of other established primary glioma cell lines. Grube *et al.* [20] established 16 of 34 GB cell lines that exhibited a spindle-form or polygonal-to-amorphous morphology and grew as a monolayer. In the present study, we also investigated cell morphology by labeling cytoskeleton components (using the phalloidin probe). The cells exhibited a morphology similar to those observed by light microscopy. Interestingly, the presence of rounder rather than polygonal cells was noted.

The differences observed in morphology may be related to the time at which the cells were imaged, as phalloidin labeling was performed in the initial weeks of culture, whereas light microscopy was conducted after establishment. Machado *et al.* [11] observed a similar pattern during GB (NG97) establishment: in the first passages, GB cultures grew more slowly and presented a more rounded shape. At the 13<sup>th</sup> passage, dendritic-like cells, with more extensive cytoplasmic extensions, appeared in the culture. Subsequently, spindle-shaped cells appeared as the culture became dense. We hypothesize that these differences may be related to the heterogeneity of the tumor and the slow adaptation of the cells to a new environment. Cells may create more connections during

culture, forming additional cellular extensions that connect to one another as they adapt to the new environment. Despite the GB (C03) cell line growing faster at the beginning of culture, its morphology remained similar to the other astrocytic (N07 and L09) cell lines. In addition to morphological analyses, to characterize and confirm the established cell lines as astrocytoma and GB, immunofluorescence staining for GFAP was performed. GFAP, a protein involved in the structure and function of the cytoskeleton, is commonly used as a marker of astrocytes [21,22]. Our results indicated that the three HGGs were positive for GFAP, confirming their astrocytic origin. Furthermore, for the validation of the cell lines, it was also important to evaluate whether the cell lines maintained the ability to form tumors. Studies report that the implantation of tumor cell lines in mice does not always lead to tumor development [21]. However, this is an important factor to reliably attest to the tumorigenicity of new tumor cell lines. In the present study, all three HGG cell lines were tumorigenic in RAG-/- C57BL6 mice, indicating that the cells are neoplastic and malignant. Histopathological analysis of xenograft tumors from all three cell lines revealed increased cellularity, variation in nuclear size, and mitotic figures. These characteristics are in line with other studies describing malignant astrocytoma tumors, which are distinguished by high mitotic activity and increased cellularity [23,24]. The difference in size and weight of the tumors obtained did not influence the histopathological analyses, which were very similar, despite being from three different cell lines.

## 5. Conclusion

Three HGG cell lines (C03, N07, and L09) obtained from different patients were successfully established. Characterization confirmed their astrocytic origin, and validation in a xenograft murine model demonstrated their ability to form tumors post-establishment. Therefore, these newly established cell lines prove to be useful for studying cell and molecular biology, as well as for the development of new glioma treatments.

## Acknowledgments

We would like to thank the support and the access to equipment provided by the National Institute of Science and Technology on Photonics Applied to Cell Biology (INFABIC) at the State University of Campinas. Figure 1 was created using BioRender (BioRender.com).

## Funding

This study was financed by the São Paulo Research Foundation (FAPESP; #2019/10003-3 [Natália Barreto's scholarship], #2022/03543-4, and #2015/04194-0), the National Council for Scientific and Technological Development (Conselho Nacional de Desenvolvimento Científico e Tecnológico [CNPq]; 148156/2019-3 [Natália Barreto's scholarship]), and the Education, Research, and Extension Support Fund (Fundo de Apoio ao Ensino, à Pesquisa e à Extensão [FAEPEX/UNICAMP]; #2588/20, #2124/21, #2569/21, #2389/22,

#2768/22, #3515/23, and #3462/23). INFABIC is co-funded by FAPESP (#2014/50938-8) and CNPq (#465699/2014-6).

### Conflicts of Interest

The authors declare no conflicts of interest.

### Ethics Approval and Consent to Participate

All methods and experiments were performed strictly following the guidelines of the Research Ethics Committee from the University of Campinas (UNICAMP - Campinas, São Paulo, Brazil): CAAE: 15215219.5.0000.5404, and from the Central Hospital of Santa Casa (São Paulo, Brazil): CAAE: 15215219.5.3001.5479. Animal experimentation was carried out following the Ethical Principles on Animal Research, adopted by the Brazilian College of Animal Experimentation (Colégio Brasileiro de Experimentação Animal, COBEA), and approved by the Ethics Committee on the Use of Animals (CEUA/UNICAMP; 6200-1/2023). All authors provided consent for publication.

### Consent for Publication

Tissue samples were obtained after informed patient consent (Informed Consent Form [TCLE]). By signing the TCLE, patients agreed to disclose images and data for research purposes.

### Availability of Data

Data are available from the corresponding author upon reasonable request.

### References

- [1] Ostrom QT, Cioffi G, Gittleman H, Patil N, Waite K, Kruchko C, *et al.* CBTRUS Statistical Report: Primary Brain and Other Central Nervous System Tumors Diagnosed in the United States in 2012-2016. *Neuro Oncol* 2019;21:v1-100. doi: 10.1093/neuonc/noz150
- [2] Louis DN, Perry A, Wesseling P, Brat DJ, Cree IA, Figarella-Branger D, *et al.* The 2021 WHO Classification of Tumors of the Central Nervous System: A summary. *Neuro Oncol* 2021;23:1231-51. doi: 10.1093/neuonc/noab106
- [3] Barreto Dos Santos N, Bonfanti AP, da Rocha-E-Silva TA, Da Silva PI Jr., Da Cruz-Höfling MA, Verinaud L, *et al.* Venom of the *Phoneutria nigriventer* Spider Alters the CELL Cycle, Viability, and Migration of Cancer Cells. *J Cell Physiol* 2019;234:1398-415. doi: 10.1002/jcp.26935
- [4] Higginbottom SL, Tomaskovic-Crook E, Crook JM. Considerations for Modelling Diffuse High-grade Gliomas and Developing Clinically Relevant Therapies. *Cancer Metastasis Rev* 2023;42:507-41. doi: 10.1007/s10555-023-10100-7
- [5] Stupp R, Mason WP, van den Bent MJ, Weller M, Fisher B, Taphoorn MJ, *et al.* Radiotherapy Plus Concomitant and Adjuvant Temozolomide for Glioblastoma. *N Engl J Med* 2005;352:987-96. doi: 10.1056/NEJMoa043330
- [6] Rapôso C, Vitorino-Araujo JL, Barreto N. Molecular Markers of Gliomas to Predict Treatment and Prognosis: Current State and Future Directions. In: Brain Tumor Center of Excellence, Wake Forest Baptist Medical Center Comprehensive Cancer Center, Winston Salem, NC, USA, Debinski W, editors. *Gliomas*. Australia: Exon Publications; 2021. p. 171-86. doi: 10.36255/exonpublications.gliomas.2021.chapter10
- [7] Ostrom QT, Gittleman H, Farah P, Ondracek A, Chen Y, Wolinsky Y, *et al.* CBTRUS Statistical Report: Primary Brain and Central Nervous System Tumors Diagnosed in the United States in 2006-2010. *Neuro Oncol* 2013;15:ii1-56. doi: 10.1093/neuonc/not151
- [8] Tan AC, Ashley DM, López GY, Malinzak M, Friedman HS, Khasraw M. Management of Glioblastoma: State of the Art and Future Directions. *CA Cancer J Clin* 2020;70:299-312. doi: 10.3322/caac.21613
- [9] Barretina J, Caponigro G, Stransky N, Venkatesan K, Margolin AA, Kim S, *et al.* The Cancer Cell Line Encyclopedia Enables Predictive Modelling of Anticancer Drug Sensitivity. *Nature* 2012;483(7391):603-7. doi: 10.1038/nature11003
- [10] Huo KG, D'Arcangelo E, Tsao MS. Patient-derived Cell Line, Xenograft and Organoid Models in Lung Cancer Therapy. *Transl Lung Cancer Res* 2020;9:2214-32. doi: 10.21037/tlcr-20-154
- [11] Machado CM, Schenka A, Vassallo J, Tamashiro WM, Gonçalves EM, Genari SC, *et al.* Morphological Characterization of a Human Glioma Cell Line. *Cancer Cell Int* 2005;5:13. doi: 10.1186/1475-2867-5-13
- [12] Grippo MC, Penteado PF, Carelli EF, Cruz-Höfling MA, Verinaud L. Establishment and Partial Characterization of a Continuous Human Malignant Glioma Cell Line: NG97. *Cell Mol Neurobiol* 2001;21:421-8. doi: 10.1023/a:1012662423863
- [13] Barreto N, Caballero M, Bonfanti AP, de Mato FC, Munhoz J, da Rocha-E-Silva TA, *et al.* Spider Venom Components Decrease Glioblastoma Cell Migration and Invasion through RhoA-ROCK and Na<sup>+</sup>/K<sup>+</sup>-ATPase  $\beta$ 2: Potential Molecular Entities to Treat Invasive Brain Cancer. *Cancer Cell Int* 2020;20:576. doi: 10.1186/s12935-020-01643-8
- [14] Bonfanti AP, Barreto N, Munhoz J, Caballero M, Cordeiro G, Rocha-E-Silva T, *et al.* Spider Venom Administration Impairs Glioblastoma Growth and



- Modulates Immune Response in a Non-clinical Model. *Sci Rep* 2020;10:5876.  
doi: 10.1038/s41598-020-62620-9
- [15] Caballero M, Barreto N, Bonfanti AP, Munhoz J, Rocha-E-Silva T, Sutti R, *et al.* Isolated Components From Spider Venom Targeting Human Glioblastoma Cells and Its Potential Combined Therapy With Rapamycin. *Front Mol Biosci* 2022;9:752668.  
doi: 10.3389/fmolb.2022.752668
- [16] De Mato FC, Barreto N, Cordeiro G, Munhoz J, Bonfanti AP, Da Rocha-E-Silva TA, *et al.* Isolated Peptide from Spider Venom Modulates Dendritic Cells *In Vitro*: A Possible Application in Oncoimmunotherapy for Glioblastoma. *Cells* 2023;12:1023.  
doi: 10.3390/cells12071023
- [17] Bian X, Cao F, Wang X, Hou Y, Zhao H, Liu Y. Establishment and Characterization of a New Human Colon Cancer Cell Line, PUMC-CRC1. *Sci Rep* 2021;11:13122.  
doi: 10.1038/s41598-021-92491-7
- [18] Feng F, Huang C, Xiao M, Wang H, Gao Q, Chen Z, *et al.* Establishment and Characterization of Patient-derived Primary Cell Lines as Preclinical Models for Gallbladder Carcinoma. *Transl Cancer Res* 2020;9:1698-710.  
doi: 10.21037/tcr.2020.02.04
- [19] Gillet JP, Calcagno AM, Varma S, Marino M, Green LJ, Vora MI, *et al.* Redefining the Relevance of Established Cancer Cell Lines to the Study of Mechanisms of Clinical Anti-cancer Drug Resistance. *Proc Natl Acad Sci U S A* 2011;108:18708-13.  
doi: 10.1073/pnas.1111840108
- [20] Grube S, Freitag D, Kalff R, Ewald C, Walter J. Characterization of Adherent Primary Cell Lines From Fresh Human Glioblastoma Tissue, Defining Glial Fibrillary Acidic Protein as a Reliable Marker in Establishment of Glioblastoma Cell Culture. *Cancer Rep Hoboken* 2021;4:e1324.  
doi: 10.1002/cnr2.1324
- [21] Cheng F, Wan X, Wang B, Li Y, Peng P, Xu S, *et al.* Establishment and Characteristics of GWH04, A New Primary Human Glioblastoma Cell Line. *Int J Oncol* 2022;61:139.  
doi: 10.3892/ijo.2022.5429
- [22] Brenner M, Messing A. Regulation of GFAP Expression. *ASN Neuro* 2021;13:1-32.  
doi: 10.1177/1759091420981206
- [23] Wood MD, Halfpenny AM, Moore SR. Applications of Molecular Neuro-oncology - A Review of Diffuse Glioma Integrated Diagnosis and Emerging Molecular Entities. *Diagn Pathol* 2019;14:29.  
doi: 10.1186/s13000-019-0802-8
- [24] Ferris SP, Hofmann JW, Solomon DA, Perry A. Characterization of Gliomas: From Morphology to Molecules. *Virchows Arch* 2017;471:257-69.  
doi: 10.1007/s00428-017-2181-4

#### Publisher's note

AccScience Publishing remains neutral with regard to jurisdictional claims in published maps and institutional affiliations.